

We are IntechOpen, the world's leading publisher of Open Access books Built by scientists, for scientists

6,900

Open access books available

186,000

International authors and editors

200M

Downloads

Our authors are among the

154

Countries delivered to

TOP 1%

most cited scientists

12.2%

Contributors from top 500 universities



WEB OF SCIENCE™

Selection of our books indexed in the Book Citation Index
in Web of Science™ Core Collection (BKCI)

Interested in publishing with us?
Contact book.department@intechopen.com

Numbers displayed above are based on latest data collected.
For more information visit www.intechopen.com



Power Quality Problems Generated by Line Frequency Coreless Induction Furnaces

Angela Iagăr
Politehnica University Timișoara
Romania

1. Introduction

The increased problems in power networks impose to identify the sources of power quality deterioration. The most important parameters which affect power quality are harmonics, voltage instability and reactive power burden (Arrillaga et al., 2000). They cause low system efficiency, poor power factor, cause disturbance to other consumers and interference in the nearly communication networks (Lattarulo, 2007; De la Rosa, 2006; Muzi, 2008).

In induction melting is noticed mainly the efficiency, high heating rate and the reduced oxidation level of the processed material, the improved work conditions and the possibility of an accurate control of the technological processes (Rudnev et al., 2002).

Induction heating equipments do not introduce dust and noise emissions in operation, but cause power quality problems in the electric power system (Nuns et al., 1993).

Induction-melt furnaces supplies by medium frequency converters generate fixed and variable frequency harmonics. Both current and voltage-fed inverters generate harmonics back into power lines in the process of rectifying AC to DC (EPRI, 1999).

Harmonics flowing in the network causing additional losses and decreasing the equipments lifetime. Also, the harmonics can interfere with control, communication or protection equipments (Arrillaga et al., 2000; George & Agarwal, 2008).

In addition to the harmonics that are normally expected from different pulse rectifiers, large furnaces operating at a few hundred hertz can generate interharmonics (EPRI, 1999). Interharmonics can overload power system capacitors, introduce noise into transformers, cause lights to flicker, instigate UPS alarms, and trip adjustable-speed drives.

High-frequency systems, which operate at greater than 3 kHz are relatively small and limited to special applications. Electromagnetic pollution produced by the operation of these equipments is small.

The induction furnaces supplied at line frequency (50 Hz) are of high capacity and represent great power consumers.

Being single-phase loads, these furnaces introduce unbalances that lead to the increasing of power and active energy losses in the network. In case of channel furnaces it was found the presence of harmonics in the current absorbed from the power supply network. These harmonics can be determined by the non-sinusoidal supply voltages or the load's nonlinearity, owed to the saturation of the magnetic circuit (Nuns et al., 1993).

This chapter presents a study about power quality problems introduced by the operation of line frequency coreless induction furnaces. The specialty literature does not offer detailed information regarding the harmonic distortion in the case of these furnaces.

2. Electrical installation of the induction-melt furnace

The analyzed coreless induction furnace has 12.5 t capacity of cast-iron; the furnace is supplied from the three-phase medium-voltage network (6 kV) through a transformer in Δ/Y connection, with step-variable voltage. Load balancing of the three-phase network is currently achieved by a Steinmetz circuit, and the power factor correction is achieved by means of some step-switching capacitor banks (fig.1).

In the electric scheme from fig. 1: Q_1 is an indoor three-poles disconnecter, type STIm-10-1250 (10 kV, 1250 A), Q_2 is an automatic circuit-breaker OROMAX (6 kV, 2500 A), T is the furnace transformer (2625 kVA; 6/1.2 kV), K_1 is a contactor (1600 A), (1) is the Steinmetz circuit used to balance the line currents, (2) is the power factor compensation installation, TC_{1m} , TC_{2m} , TC_{3m} (300/5 A) and TC_1 , TC_2 , TC_3 (1600/5 A) are current transformers, TT_{1m} (6000/100 V), TT_1 (1320/110 V) are voltage transformers, and M is the flexible connection of the induction furnace CI.

Within the study the following physical aspects were taken into account:

- induction heating of ferromagnetic materials involve complex and strongly coupled phenomena (generating of eddy currents, heat transfer, phase transitions and mechanical stress of the processed material);
- the resistivity of cast-iron increases with temperature;
- the relative magnetic permeability of the cast-iron changes very fast against temperature near to the Curie point (above the Curie temperature the cast-iron becomes paramagnetic).

As consequence, will be present the influence of the following factors upon the energetic parameters of the installation: furnace charge, furnace supply voltage, load balancing installation and the one of power factor compensation.

3. Measured signals in electrical installation of the induction furnace

The measurements have been made both in the secondary (Low Voltage Line - LV Line) and in the primary (Medium Voltage Line - MV Line) of the furnace transformer, using the CA8334 three-phase power quality analyzer. CA8334 gave an instantaneous image of the main characteristics of power quality for the analyzed induction furnace. The main parameters measured by the CA8334 analyser were: TRMS AC phase voltages and TRMS AC line currents; peak voltage and current; active, reactive and apparent power per phase; harmonics for voltages and currents up to the 50th order (CA8334, technical handbook, 2007).

CA8334 analyser provide numerous calculated values and processing functions in compliance with EMC standards in use (EN 50160, IEC 61000-4-15, IEC 61000-4-30, IEC 61000-4-7, IEC 61000-3-4).

The most significant moments during the induction melting process of the cast-iron charge were considered:

- cold state of the charge (after 15 minutes from the beginning of the heating process);
- intermediate state (after 5 hours and 40 minutes from the beginning of the heating process);
- the end of the melting (after 8 hours from the beginning of the heating process).

Further are presented the waveforms and harmonic spectra of the phase voltages and line currents measured during the heating of the charge (Iagăr et al, 2009).

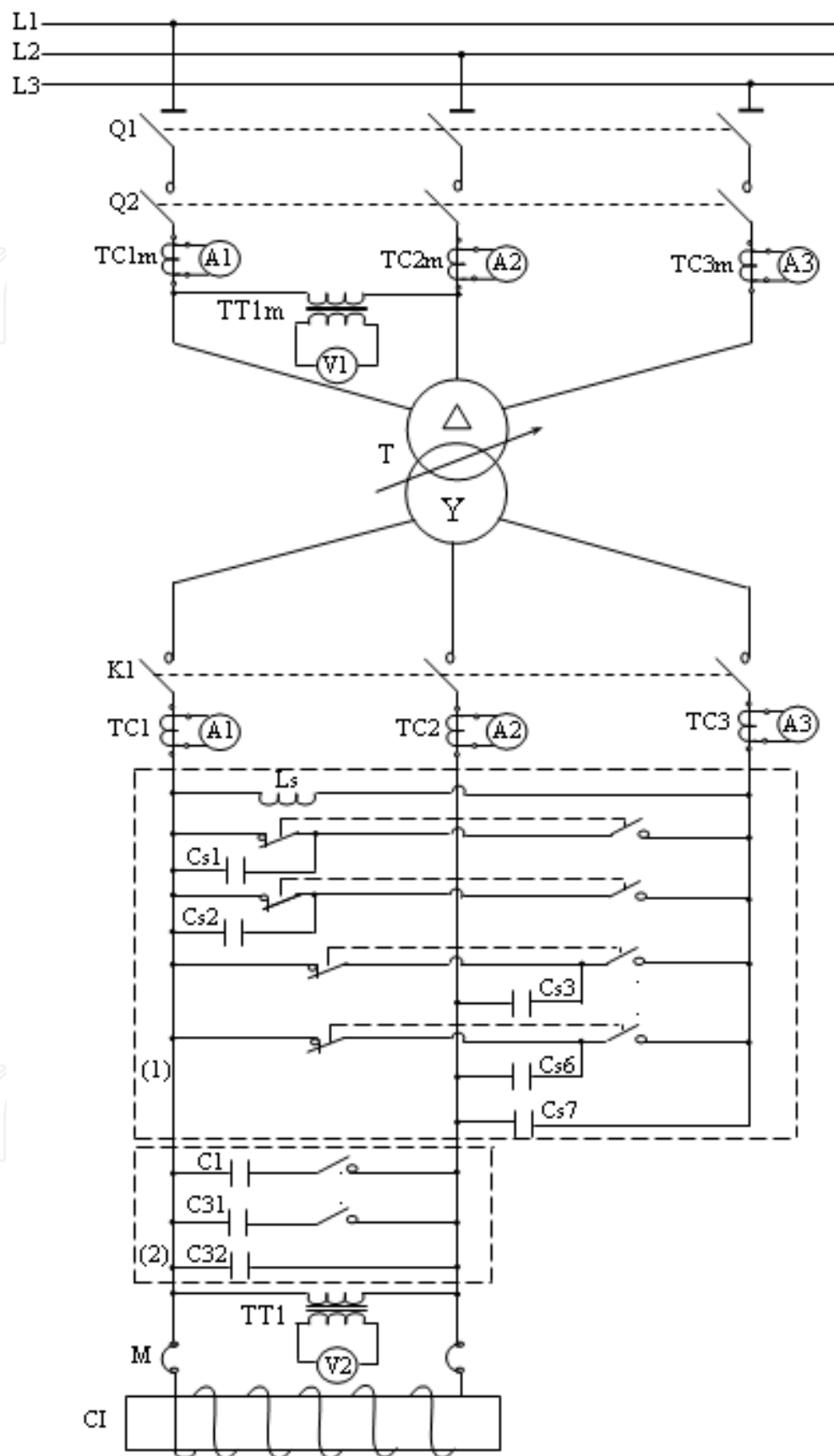


Fig. 1. Electric scheme of the analyzed furnace

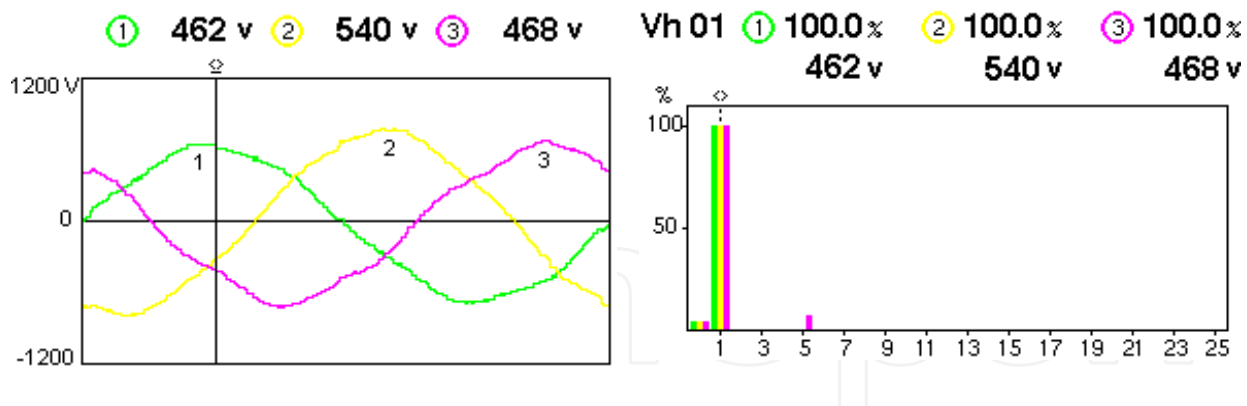


Fig. 2. Waveforms and harmonic spectra of the phase voltages in the cold state of the charge (LV Line)

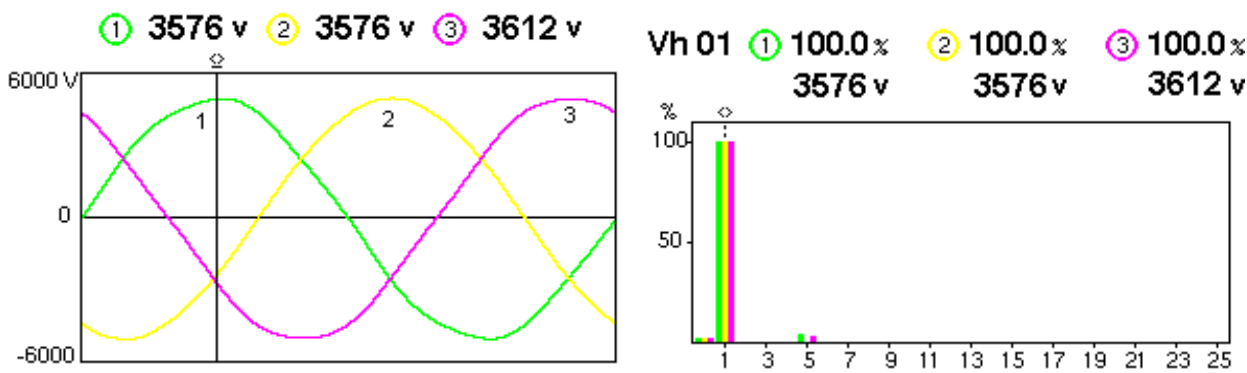


Fig. 3. Waveforms and harmonic spectra of the phase voltages in the cold state of the charge (MV Line)

In the first heating stage, the electromagnetic disturbances of the phase voltages on LV Line and on MV Line are very small. The 5th harmonic does not exceed the compatibility limit, but the voltage interharmonics exceed the compatibility limits (IEC 61000-3-4, 1998; IEC/TR 61000-3-6, 2005).

On MV Line the current I_2 was impossible to be measured because the CA8334 three-phase power quality analyser was connected to the watt-hour meter input. The watt-hour meter had three voltages (U_{12} , U_{23} , U_{31}) and two currents (I_1 and I_3).

Waveform distortion of the currents in cold state is large (fig. 4, 5). At the beginning of the cast-iron heating the 3rd, 5th, 7th, 9th, 11th, 13th, 15th harmonics and even harmonics (2nd, 4th, 6th, 8th) are present in the currents on the LV Line. The 5th and 15th harmonics exceed the compatibility limits (IEC 61000-3-4, 1998).

In the cold state the 2nd, 3rd, 5th, 7th, 9th, 11th, 13th and 15th harmonics are present in the currents absorbed from the MV Line. The 5th harmonic exceeds the compatibility limits (IEC/TR 61000-3-6, 2005).

In the intermediate state, part of the charge is heated above the Curie temperature and becomes paramagnetic, and the rest of the charge still has ferromagnetic properties. The furnace charge is partially melted.

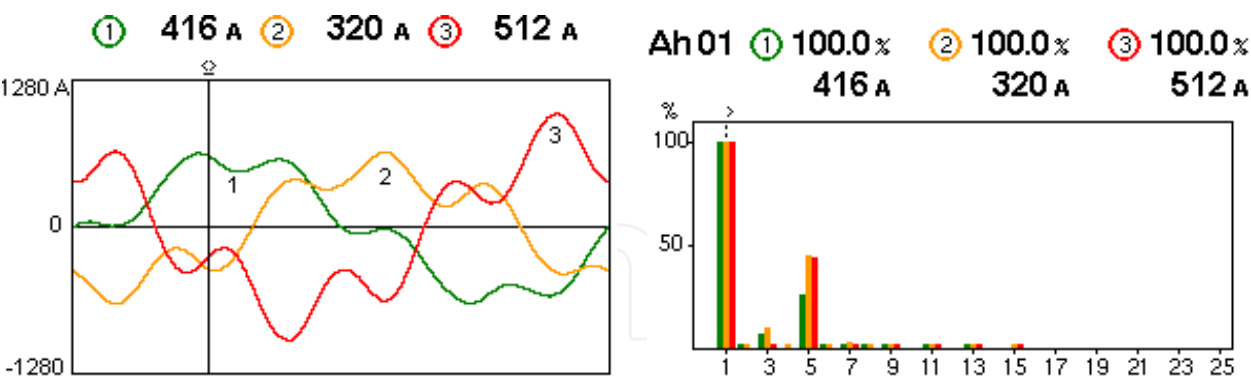


Fig. 4. Waveforms and harmonic spectra of the line currents in the cold state of the charge (LV Line)

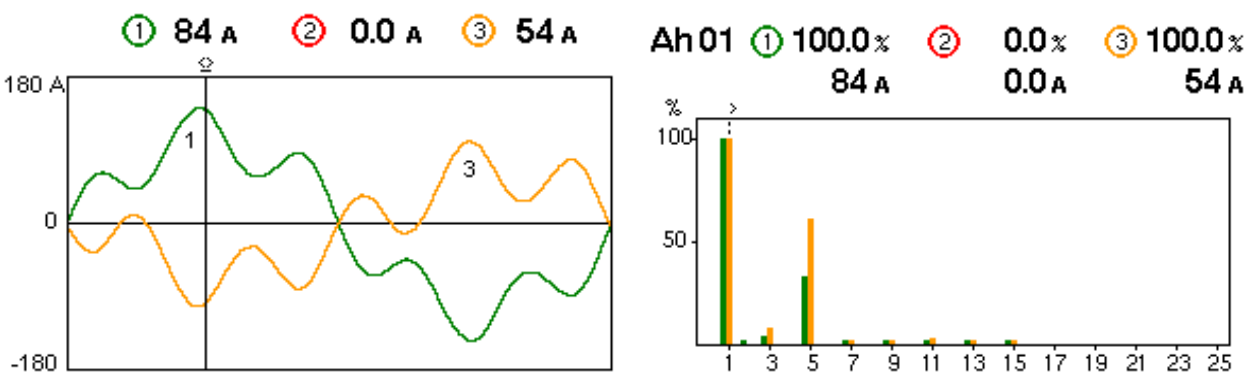


Fig. 5. Waveforms and harmonic spectra of the line currents in the cold state of the charge (MV Line)

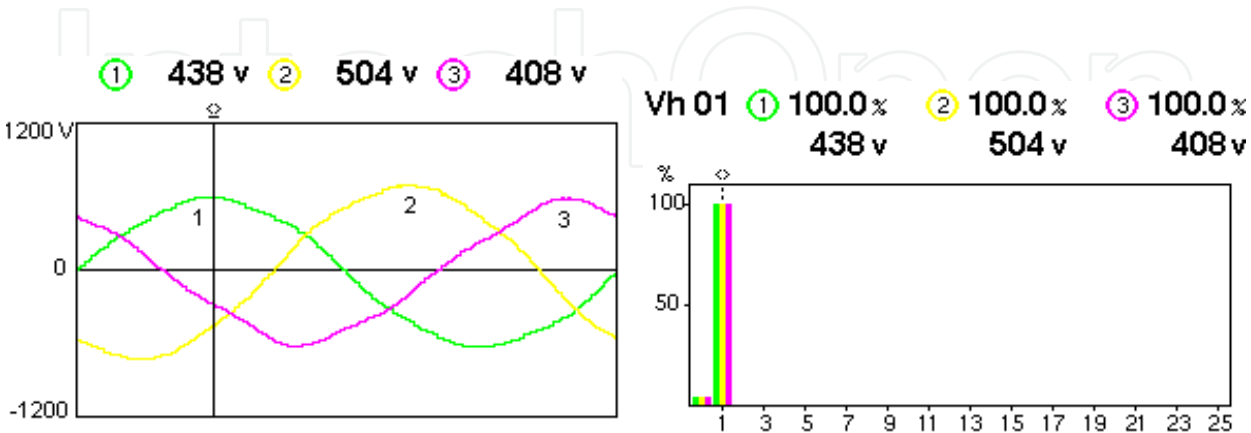


Fig. 6. Waveforms and harmonic spectra of the phase voltages in the intermediate state (LV Line)

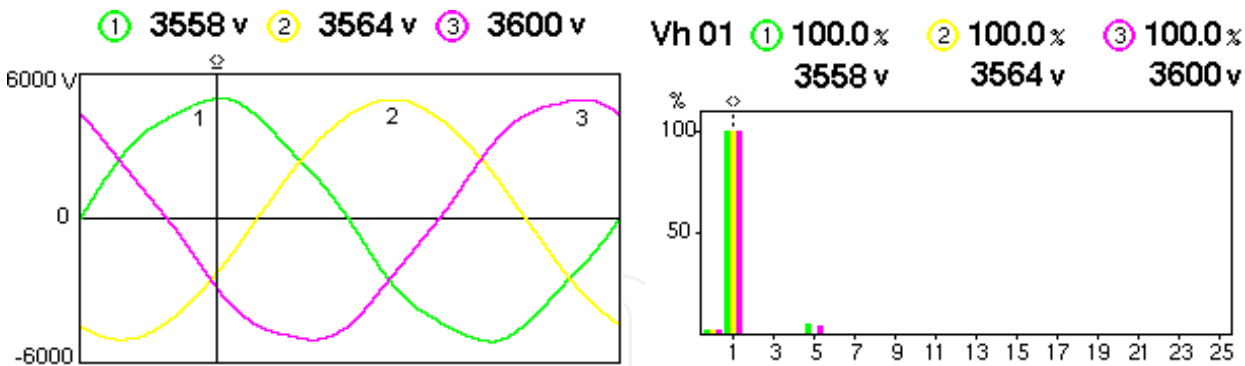


Fig. 7. Waveforms and harmonic spectra of the voltages in the intermediate state (MV Line)

In the intermediate state of the charge, the voltage interharmonics exceed the compatibility limits. The 5th harmonic do not exceeds the compatibility limits.

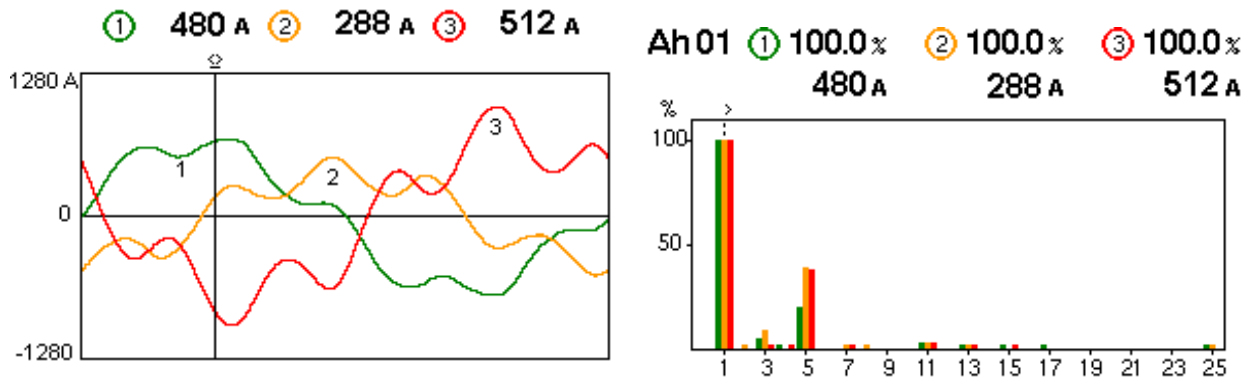


Fig. 8. Waveforms and harmonic spectra of the currents in the intermediate state (LV Line)

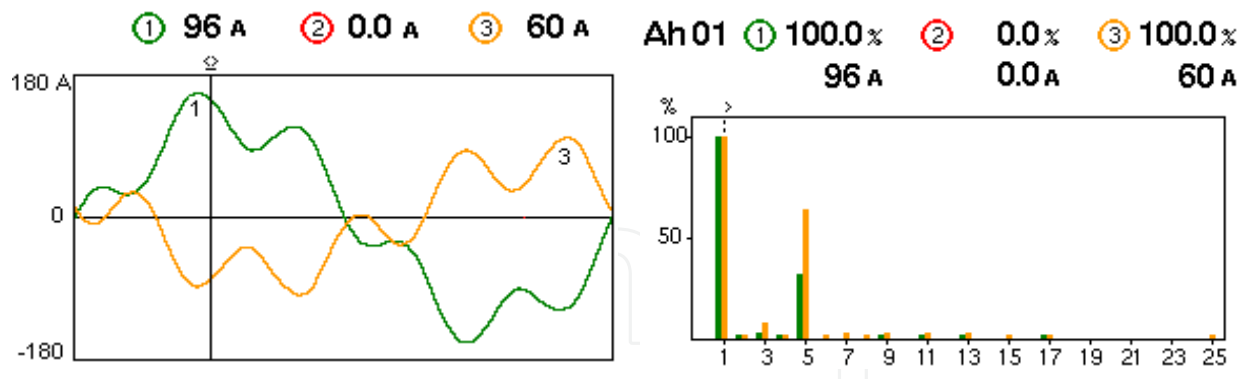


Fig. 9. Waveforms and harmonic spectra of the currents in the intermediate state (MV Line)

In the intermediate state, harmonic spectra of the currents absorbed from the LV Line present the 3rd, 5th, 7th, 11th, 13th, 15th, 17th, 25th harmonics and even harmonics (2nd, 4th, 8th). The 5th, 15th, 17th and 25th harmonics exceed the compatibility limits (IEC 61000-3-4, 1998). On MV Line, harmonic spectra of the currents present the 3rd, 5th, 7th, 9th, 11th, 13th, 15th, 17th, 25th harmonics and even harmonics (2nd, 4th, 6th, 8th). The 5th and 25th harmonics exceed the compatibility limits (IEC/TR 61000-3-6, 2005). After 8 hours from the beginning of the heating process the furnace charge is totally melted, being paramagnetic.

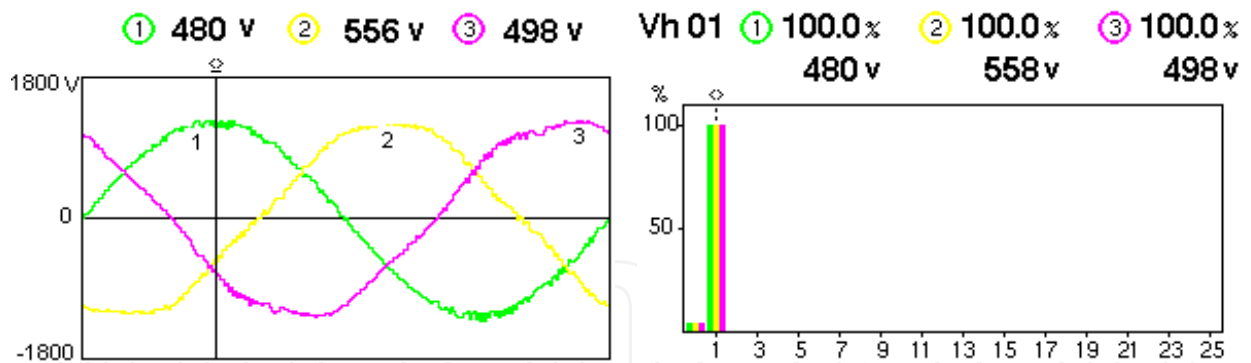


Fig. 10. Waveforms and harmonic spectra of the phase voltages at the end of the melting process (LV Line)

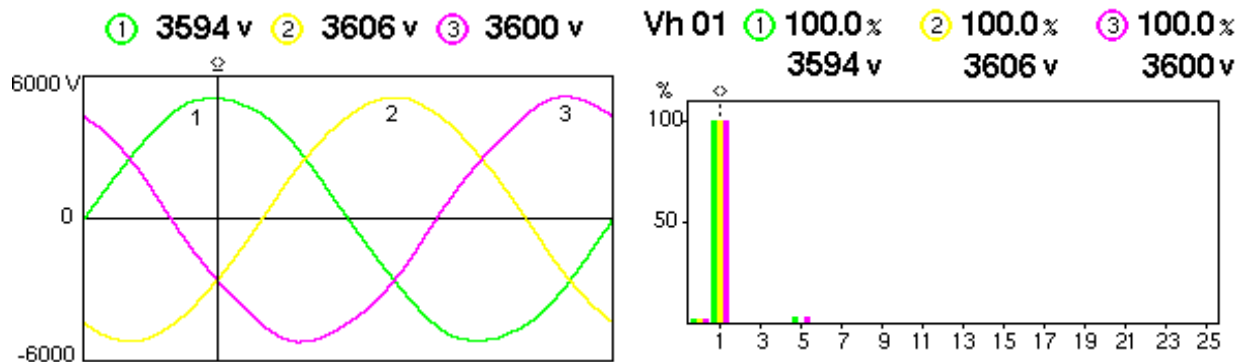


Fig. 11. Waveforms and harmonic spectra of the phase voltages at the end of the melting process (MV Line)

At the end of the melting process, the electromagnetic disturbances of the phase voltages are very small. Voltage interharmonics exceed the compatibility limits. The 5th harmonic is within compatibility limits (IEC 61000-3-4, 1998; IEC/TR 61000-3-6, 2005).

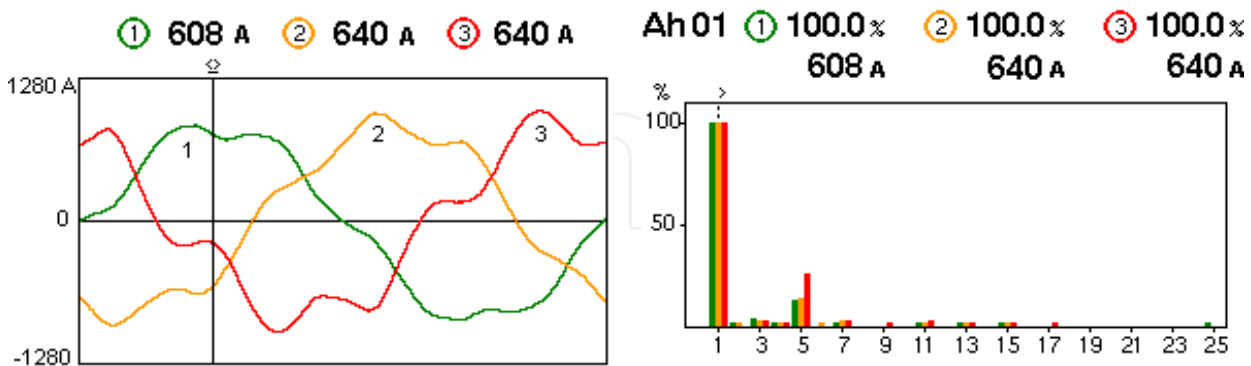


Fig. 12. Waveforms and harmonic spectra of the line currents at the end of the melting process (LV Line)

Waveform distortion of the currents at the end of the melting process is smaller than in cold state, or intermediate state. On LV Line, harmonic spectra of the currents show the presence of 3rd, 5th, 7th, 9th, 11th, 13th, 15th, 17th, 25th harmonics and even harmonics (2nd, 4th, 6th). The 5th, 15th and 25th harmonics exceed the compatibility limits (IEC 61000-3-4, 1998).

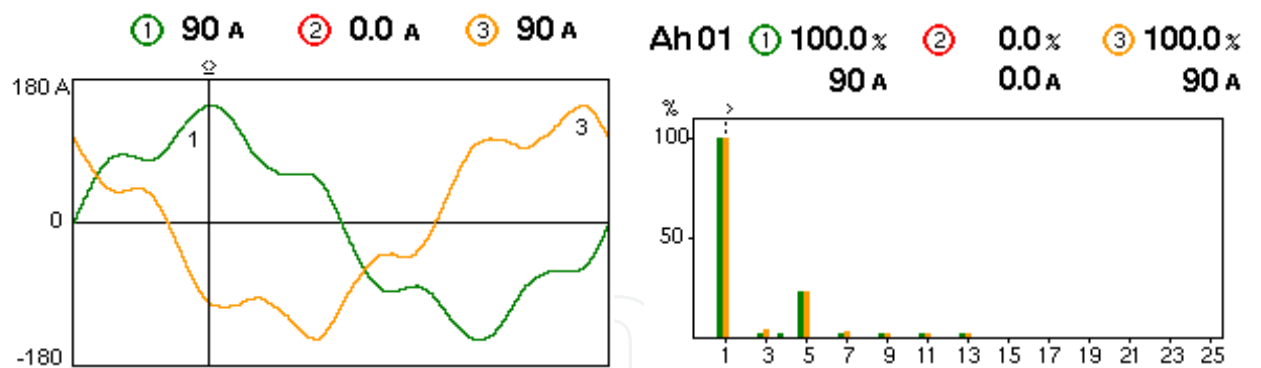


Fig. 13. Waveforms and harmonic spectra of the line currents at the end of the melting process (MV Line)

On MV Line, harmonic spectra of the currents show the presence of 3rd, 4th, 5th, 7th, 9th, 11th, 13th harmonics at the end of the melting. The 5th harmonic exceeds the compatibility limits (IEC/TR 61000-3-6, 2005). Fig.14-16 show the values of voltage and current unbalance on LV Line, in all the heating stages.

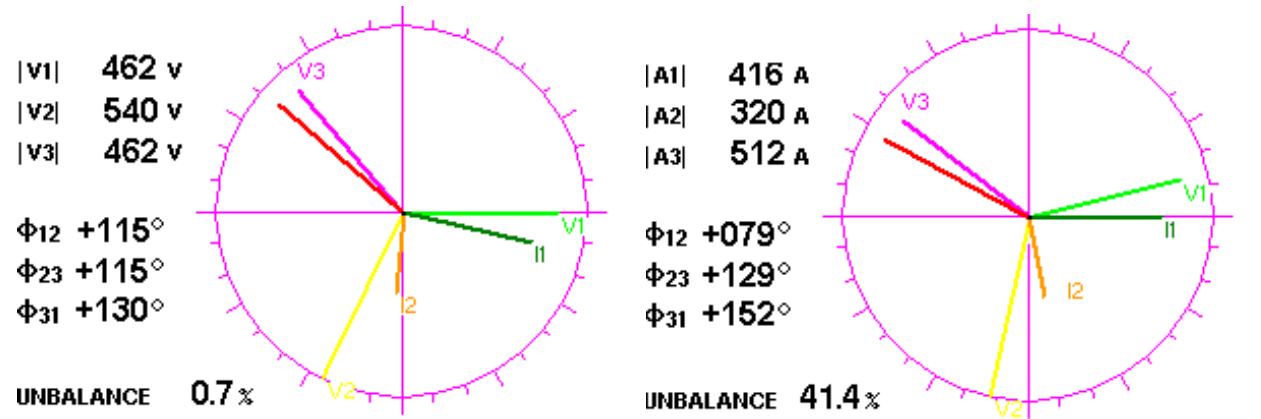


Fig. 14. Unbalance of the phase voltages and line currents in the cold state of the charge (LV Line)

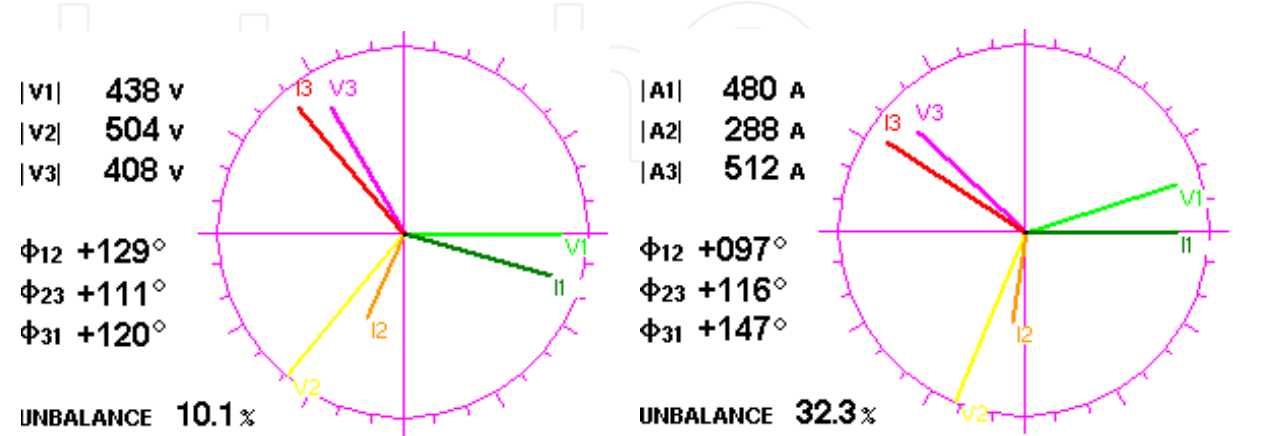


Fig. 15. Unbalance of the phase voltages and line currents in the intermediate state of the charge (LV Line)

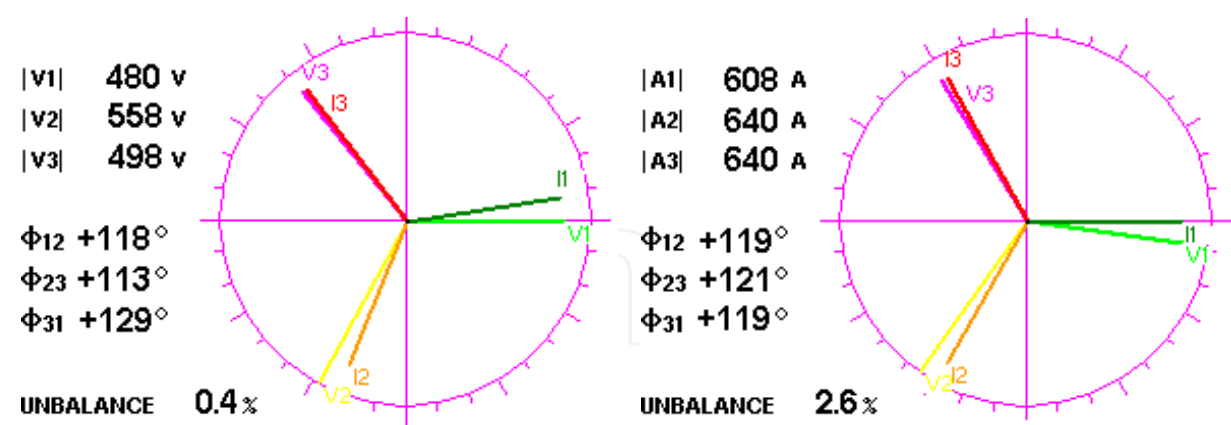


Fig. 16. Unbalance of the phase voltages and line currents at the end of the melting process (LV Line)

Voltage unbalance exceeds the permitted values in intermediate state. Current unbalance is very large in the cold state and decreases as the furnace charge is melting down.

4. The values computed by the CA8334 analyser

The values computed by the CA8334 analyser are: total harmonic distortion of voltages and currents, distortion factor of voltages and currents, K factor for current, voltage and current unbalance, power factor and displacement factor, extreme and average values for voltage and current, peak factors for current and voltage (CA8334, technical handbook, 2007). Mathematical formulae used to compute the total harmonic distortion (THD) of voltages and currents are:

$$VTHD_i = \frac{\sqrt{\sum_{n=2}^{50} (V_{harm\ ni})^2}}{V_{harm\ 1i}} \cdot 100 \tag{1}$$

$$ITHD_i = \frac{\sqrt{\sum_{n=2}^{50} (I_{harm\ ni})^2}}{I_{harm\ 1i}} \cdot 100 \tag{2}$$

V represents the phase voltage, I represents the line current, i represents the phase (i = 1, 2, 3) and n represents the order of harmonics.

Distortion factor (DF) of voltages and currents are computed by the formulae:

$$VDF_i = \frac{\sqrt{\frac{1}{2} \sum_{n=2}^{50} (V_{harm\ ni})^2}}{VRMS_i} \cdot 100 \tag{3}$$

$$IDF_i = \frac{\sqrt{\frac{1}{2} \sum_{n=2}^{50} (I_{harm \ ni})^2}}{IRMS_i} \cdot 100 \quad (4)$$

VRMS and IRMS represent the root mean square values (RMS values or effective values) for phase voltage and line current, computed over 1 second, and i represents the phase ($i = 1, 2, 3$). **K factor (KF)** is a weighting of the harmonic load currents according to their effects on transformer heating. **K factor** for current is computed by relation:

$$IKF_i = \frac{\sum_{n=1}^{50} n^2 \cdot (I_{harm \ ni})^2}{\sum_{n=1}^{50} (I_{harm \ ni})^2} \quad (5)$$

In the above relation I represents the line current, i represents the phase ($i = 1, 2, 3$) and n represents the order of harmonics. A K factor of 1 indicates a linear load (no harmonics); a higher K factor indicates the greater harmonic heating effects.

The unbalanced three-phase systems of voltages (or currents) can be reduce into three balanced systems: the positive (+), negative (-) and zero (0) sequence components.

The positive voltage True RMS and the negative voltage True RMS are given by the relations:

$$VRMS_+ = \frac{V_1 + aV_2 + a^2V_3}{3} \quad (6)$$

$$VRMS_- = \frac{V_1 + a^2V_2 + aV_3}{3} \quad (7)$$

where V_1, V_2, V_3 represent the phase voltages (using simplified complex) and $a = e^{j\frac{2\pi}{3}}$ is the complex operator.

The positive current True RMS and the negative current True RMS are given by the relations:

$$IRMS_+ = \frac{I_1 + aI_2 + a^2I_3}{3} \quad (8)$$

$$IRMS_- = \frac{I_1 + a^2I_2 + aI_3}{3} \quad (9)$$

where I_1, I_2, I_3 represent the line currents (using simplified complex).

Voltage and current unbalances (unb) are:

$$V_{unb} = \frac{|VRMS_-|}{|VRMS_+|} \cdot 100 \quad (10)$$

$$I_{unb} = \frac{|IRMS_{-}|}{|IRMS_{+}|} \cdot 100 \tag{11}$$

Power factor (PF) and displacement factor (DPF) are computed by relations:

$$PF_i = \frac{P_i}{S_i} \tag{12}$$

$$DPF_i = \cos \varphi_i \tag{13}$$

P_i [W] and S_i [VA] represent the active power and the apparent power per phase ($i = 1, 2, 3$); φ_i is the phase difference between the fundamental current and voltage, and i represents the phase.
Mathematical formulae used to compute the **peak factors (CF) for current and phase voltage** are:

$$VCF_i = \frac{\max(Vpp_i, |Vpm_i|)}{\sqrt{\frac{1}{N} \cdot \sum_{n=0}^{N-1} (V(n)_i)^2}} \tag{14}$$

$$ICF_i = \frac{\max(Ipp_i, |Ipm_i|)}{\sqrt{\frac{1}{N} \cdot \sum_{k=0}^{N-1} (I(k)_i)^2}} \tag{15}$$

In the relations (14), (15): Vpp is the PEAK+ of the phase voltage; Vpm is the PEAK- of the phase voltage; Ipp is the PEAK+ of the line current; Ipm is the PEAK- of the line current; i represents the phase ($i = 1, 2, 3$); N represents the number of the samples per period (between two consecutive zeros).
Peak values (PEAK+/PEAK-) for voltage (or current) represent the maximum/minimum values of the voltage (or current) for all the samples between two consecutive zeros. For a sinusoidal signal, the peak factor is equal to $\sqrt{2}$ (1.41). For a non-sinusoidal signal, the peak factor can be either greater than or less than $\sqrt{2}$. In the latter case, the peak factor signals divergent peak values with respect to the RMS value.
MIN/MAX values for voltage (or current) represent the minimum/maximum values of the half-period RMS voltage (or current). Average values (AVG) for voltage and current are computed over 1 second.

Tables 1-25 show the values computed by the CA8334 analyser on LV Line and on MV Line.

Heating moment	VTHD ₁ [%]	VTHD ₂ [%]	VTHD ₃ [%]
Cold state	0	4	5.4
Intermediate state	0	3.8	3.8
End of melting process	0	0	6.3

Table 1. Total harmonic distortion THD [%] for phase voltages (LV Line)

Heating moment	VTHD ₁ [%]	VTHD ₂ [%]	VTHD ₃ [%]
Cold state	2.2	0	1.7
Intermediate state	3.4	0	3.1
End of melting process	1.9	0	1.7

Table 2. Total harmonic distortion THD [%] for phase voltages (MV Line)

THD of the phase voltages do not exceed the compatibility limits in all the heating stages. The values of VTHD on MV Line are higher than the values of VTHD on LV Line.

Heating moment	ITHD ₁ [%]	ITHD ₂ [%]	ITHD ₃ [%]
Cold state	26.5	43	42
Intermediate state	20.1	39	35.5
End of melting process	14.9	16.7	30.3

Table 3. Total harmonic distortion THD [%] for line currents (LV Line)

Heating moment	ITHD ₁ [%]	ITHD ₃ [%]
Cold state	31	57.5
Intermediate state	34.3	68.7
End of melting process	22.7	24.3

Table 4. Total harmonic distortion THD [%] for line currents (MV Line)

ITHD exceed the limits permitted by norms in all the analyzed situations. The values of ITHD are higher on MV Line versus LV Line. Because THD of line currents exceed 20%, this indicates a significant electromagnetic pollution produced by the furnace in MV network.

Heating moment	VDF ₁ [%]	VDF ₂ [%]	VDF ₃ [%]
Cold state	0	0	0
Intermediate state	0	0	0
End of melting process	0	0	5.5

Table 5. Distortion factor DF [%] of phase voltages (LV Line)

Heating moment	VDF ₁ [%]	VDF ₂ [%]	VDF ₃ [%]
Cold state	1.9	0	1.4
Intermediate state	3.4	0	3
End of melting process	1.9	0	1.4

Table 6. Distortion factor DF [%] of phase voltages (MV Line)

Distortion factor of phase voltages is very small during the heating process of cast-iron charge. In all situations, distortion factor of phase voltages is smaller than total harmonic distortion.

Heating moment	IDF ₁ [%]	IDF ₂ [%]	IDF ₃ [%]
Cold state	21.7	46.2	32
Intermediate state	19.3	38.1	33.4
End of melting process	15.6	14.8	27.9

Table 7. Distortion factor DF [%] of line currents (LV Line)

Heating moment	IDF ₁ [%]	IDF ₃ [%]
Cold state	23.9	43.2
Intermediate state	32.2	61.8
End of melting process	22.7	23.4

Table 8. Distortion factor DF [%] of line currents (MV Line)

The values of distortion factor of line currents are very high during the heating process (Table 7 and Table 8). The values of IDF are higher on MV Line versus LV Line.

Heating moment	IKF ₁	IKF ₂	IKF ₃
Cold state	2.02	6.07	3.52
Intermediate state	1.88	4.8	4.02
End of melting process	1.59	1.58	2.93

Table 9. K factor KF [-] of line currents (LV Line)

Heating moment	IKF ₁	IKF ₃
Cold state	2.51	5.59
Intermediate state	3.54	8.7
End of melting process	2.21	2.27

Table 10. K factor KF [-] of line currents (MV Line)

K factor is greater than unity in all the heating stages. The values of K factor in the cold state and in the intermediate state are very high. This indicates the significant harmonic current content. K factor decrease at the end of the melting. Harmonics generate additional heat in the furnace transformer. If the transformer is non-K-rated, overheat possibly causing a fire, also reducing the life of the transformer.

Heating moment	PF			DPF		
	1	2	3	1	2	3
Cold state	0.96	0.84	0.93	0.98	0.93	0.99
Intermediate state	0.93	0.88	0.92	0.95	0.97	0.98
End of melting process	0.97	0.97	0.96	0.99	0.99	0.99

Table 11. PF [-] and DPF [-] per phase (1, 2, 3) on LV line

PF is less than unity in all the analyzed situations on LV Line. In the cold state and in the intermediate state, PF is less than neutral value (0.92) per phase 2.

Values	u_1	u_2	u_3
MAX [V]	552	624	558
AVG [V]	456	540	468
MIN [V]	0	0	0
PEAK+ [V]	660	786	678
PEAK- [V]	-672	-786	-726

Table 12. Extreme and average values for phase voltages in the cold state (LV line)

Values	u_1	u_2	u_3
MAX [V]	4176	4182	4158
AVG [V]	3558	3564	3600
MIN [V]	0	2862	2796
PEAK+ [V]	5034	5058	5028
PEAK- [V]	-5076	-5076	-5046

Table 13. Extreme and average values for phase voltages in the cold state (MV Line)

Values	u_1	u_2	u_3
MAX [V]	498	570	516
AVG [V]	486	564	504
MIN [V]	456	540	474
PEAK+ [V]	708	828	732
PEAK- [V]	-732	-810	-768

Table 14. Extreme and average values for phase voltages at the end of melting (LV line)

Values	u_1	u_2	u_3
MAX [V]	4140	4068	4146
AVG [V]	3594	3606	3600
MIN [V]	3558	3522	3480
PEAK+ [V]	5052	5118	5028
PEAK- [V]	-5094	-5136	-5046

Table 15. Extreme and average values for phase voltages at the end of melting (MV Line)

Tables 12-15 indicate a small unbalance of phase voltages in all the analyzed situations, on LV Line and on MV Line.

Values	i_1	i_2	i_3
MAX [A]	1150	732	1665
AVG [A]	416	224	544
MIN [A]	0	0	0
PEAK+ [A]	608	384	928
PEAK- [A]	-608	-384	-928

Table 16. Extreme and average values for line currents in the cold state (LV line)

Values	i_1	i_3
MAX [A]	96	60
AVG [A]	84	48
MIN [A]	0	0
PEAK+ [A]	138	90
PEAK- [A]	-138	-90

Table 17. Extreme and average values for line currents in the cold state (MV line)

Values	i_1	i_2	i_3
MAX [A]	1267	976	1713
AVG [A]	480	288	544
MIN [A]	0	0	0
PEAK+ [A]	704	512	992
PEAK- [A]	-704	-512	-992

Table 18. Extreme and average values for line currents in the intermediate state (LV line)

Values	i_1	i_3
MAX [A]	324	240
AVG [A]	96	60
MIN [A]	0	0
PEAK+ [A]	162	108
PEAK- [A]	-162	-102

Table 19. Extreme and average values for line currents in the intermediate state (MV line)

Values	i_1	i_2	i_3
MAX [A]	672	672	672
AVG [A]	608	640	672
MIN [A]	544	544	608
PEAK+ [A]	896	992	1088
PEAK- [A]	-896	-992	-1056

Table 20. Extreme and average values for line currents at the end of melting (LV line)

Values	i_1	i_3
MAX [A]	102	102
AVG [A]	90	90
MIN [A]	90	84
PEAK+ [A]	150	150
PEAK- [A]	-150	-150

Table 21. Extreme and average values for line currents at the end of melting (MV line)

The extreme and average values of line currents indicate a large unbalance in the cold state and in intermediate state. At the end of the melting the unbalance of currents is small.

Heating moment	VCF_1	VCF_2	VCF_3
Cold state	1.47	1.46	1.53
Intermediate state	1.48	1.44	1.56
End of melting process	1.45	1.47	1.49

Table 22. Peak factors CF [-] of phase voltages (LV Line)

Heating moment	VCF_1	VCF_2	VCF_3
Cold state	1.42	1.42	1.39
Intermediate state	1.44	1.42	1.39
End of melting process	1.45	1.47	1.49

Table 23. Peak factors CF [-] of phase voltages (MV Line)

Peak factors of phase voltages do not exceed very much the peak factor for sinusoidal signals (1.41) in all the heating stages. This indicates a small distortion of phase voltages.

Heating moment	ICF_1	ICF_2	ICF_3
Cold state	1.59	1.83	1.81
Intermediate state	1.51	1.88	1.83
End of melting process	1.48	1.64	1.66

Table 24. Peak factors CF [-] of line currents (LV Line)

Heating moment	ICF_1	ICF_3
Cold state	1.68	1.82
Intermediate state	1.72	1.79
End of melting process	1.68	1.68

Table 25. Peak factors CF [-] of line currents (MV Line)

Peak factors of line currents are between 1.48 and 1.88. This indicates that the analyzed furnace is a non-linear load. A high peak factor characterizes high transient overcurrents which, when detected by protection devices, can cause nuisance tripping.

5. Recorded parameters in the electrical installation of the induction furnace

The recorded parameters in the electrical installation of analyzed furnace are: RMS values of phase voltages and currents, total harmonic distortion of phase voltages and currents, power factor and displacement factor per phase 1, active power, reactive power and apparent power per phase 1.

Fig.17-21 show the recorded parameters on MV Line, in the first stage of the heating. In the recording period (11:20-12:18), the furnace charge was ferromagnetic.

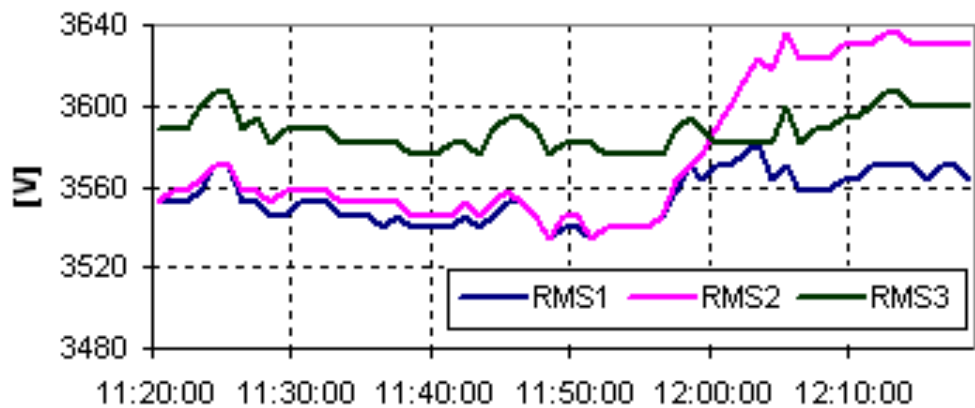


Fig. 17. RMS values of the phase voltages in the cold state (MV Line)

RMS values of phase voltages in the cold state indicate a small unbalance of the load. THD of phase voltages are within compatibility limits in the first stage of the heating process. The RMS values of line currents show a poor balance between the phases. The Steinmetz circuit is not efficient for load balancing in this stage of the melting process. THD of line currents have values of 20%...70%, and exceed very much the compatibility limits during the recording period. This indicates a significant harmonic pollution with a risk of temperature rise.

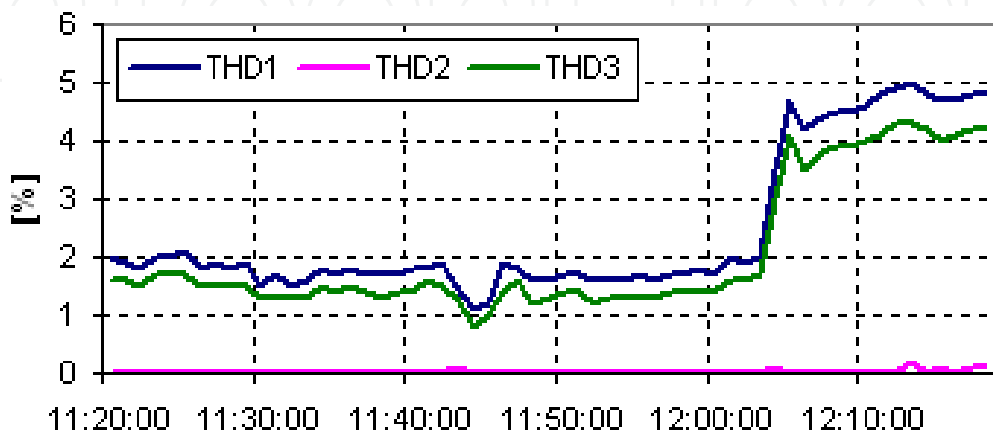


Fig. 18. THD of phase voltages in the cold state (MV Line)

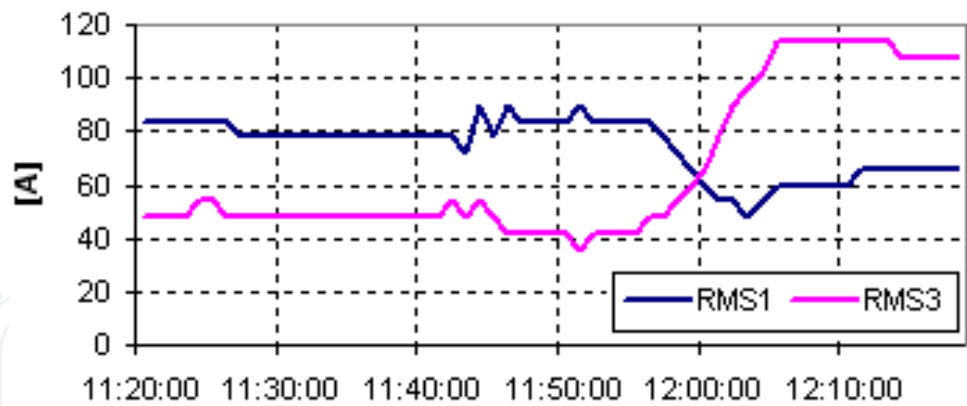


Fig. 19. RMS values of the currents in the cold state (MV Line)

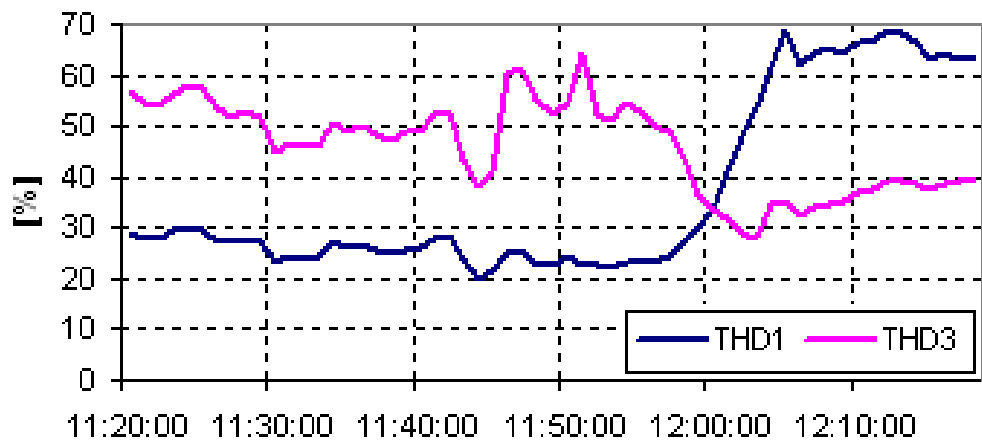


Fig. 20. THD of line currents in the cold state (MV Line)

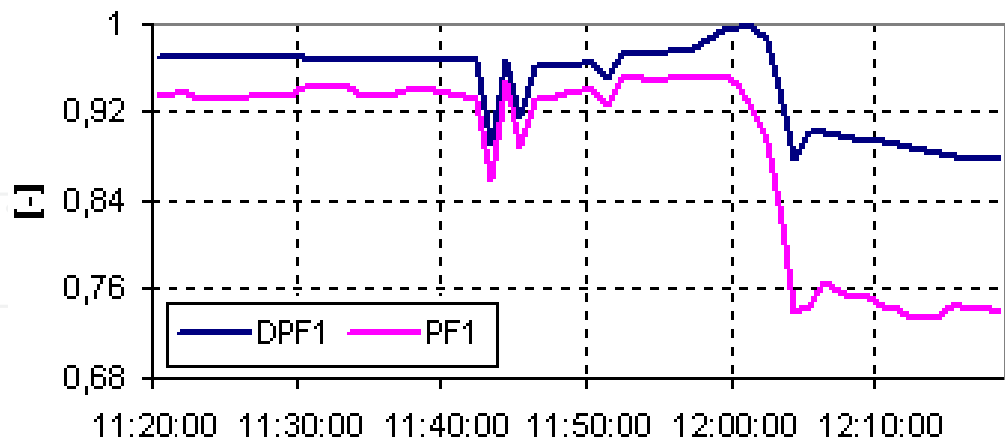


Fig. 21. DPF and PF per phase 1 in the cold state (MV Line)

In the recorded period of the cold state, power factor (PF) per phase 1 and displacement factor (DPF) per phase 1 are less than unity; in the time period 12:00 - 12:18 PF is less than neutral value (0.92). PF is smaller than DPF because PF includes fundamental reactive power and harmonic power, while DPF only includes the fundamental reactive power caused by a phase shift between voltage and fundamental current.

Fig.22-29 show the recorded parameters in the intermediate state of the heating. The furnace charge was partially melted in the recording period, 13:20-14:18.

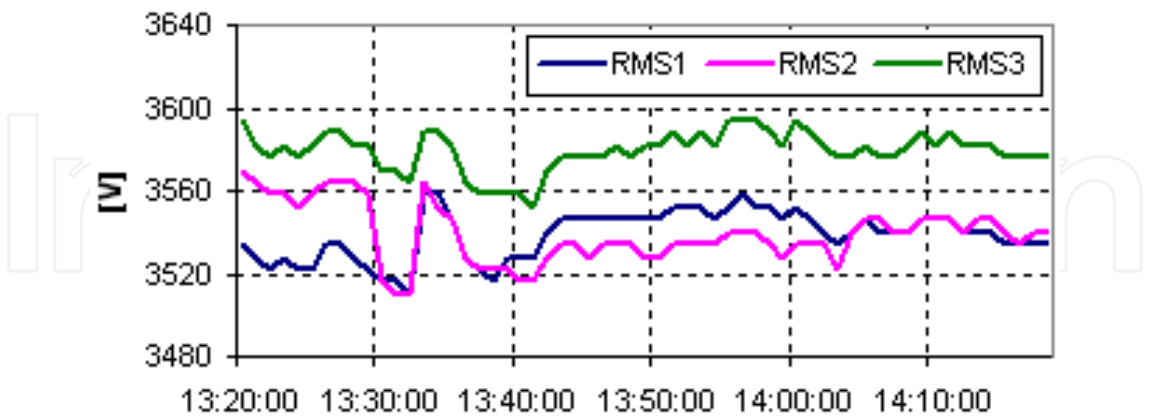


Fig. 22. RMS values of phase voltages in the intermediate state (MV Line)

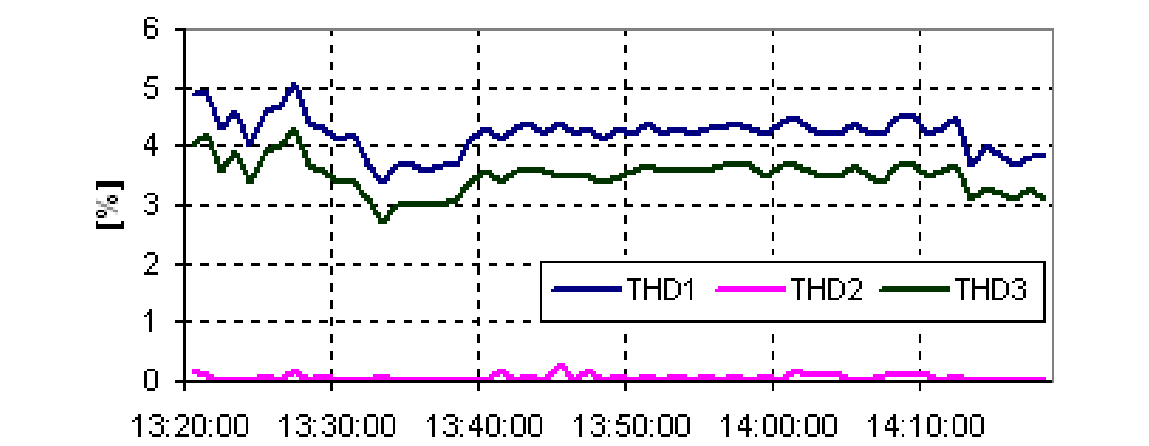


Fig. 23. THD of phase voltages in the intermediate state (MV Line)

In the intermediate state, THD of phase voltages do not exceed the compatibility limits, but are bigger comparatively with the cold state.

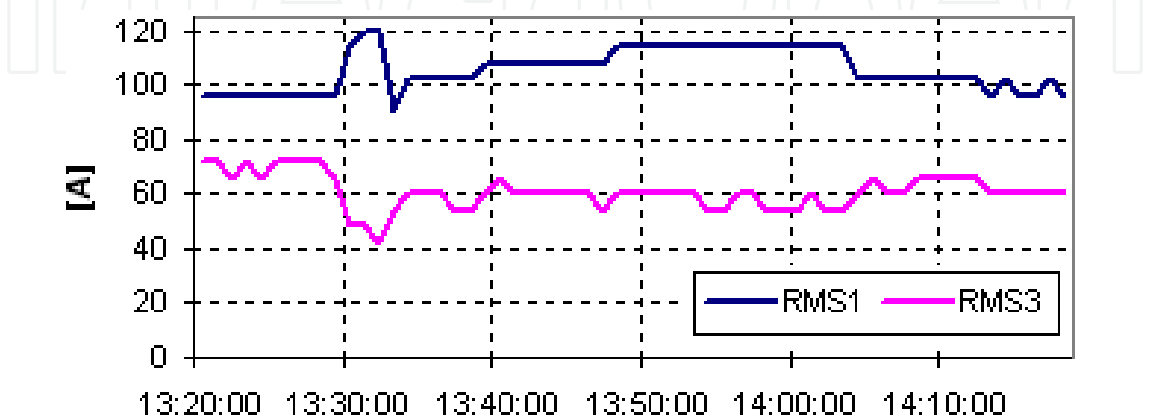


Fig. 24. RMS values of line currents in the intermediate state (MV Line)

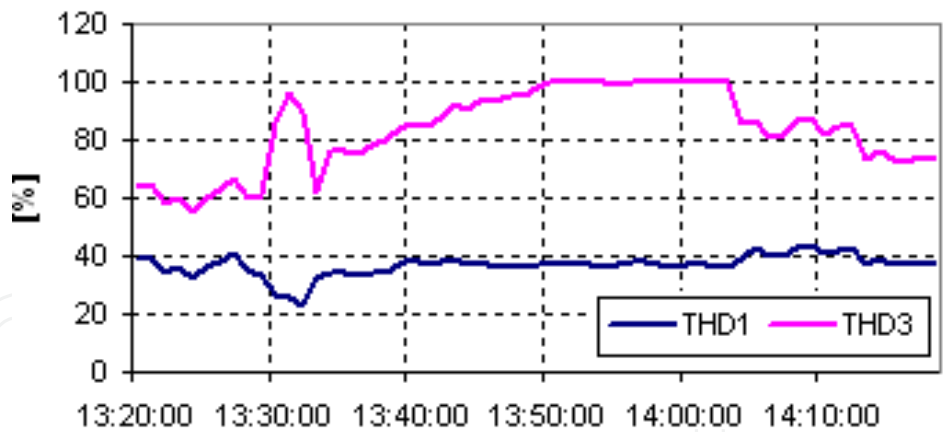


Fig. 25. THD of line currents in the intermediate state (MV Line)

In the intermediate state, the RMS values of the line currents show a poor balance between the phases. THD of line currents are remarkably high and exceed the compatibility limits.

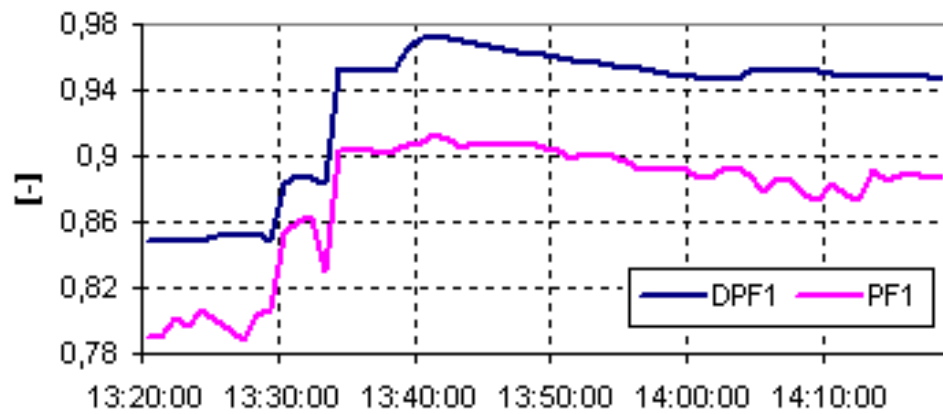


Fig. 26. DPF and PF per phase 1 in the intermediate state (MV Line)

The difference between the power factor and the displacement factor is significant in the intermediate state. This indicates the significant harmonic pollution and reactive power consumption.

PF per phase 1 is less than neutral value (0.92) almost all the time during the intermediate state. In the time period 13:20-13:35, PF is very small.

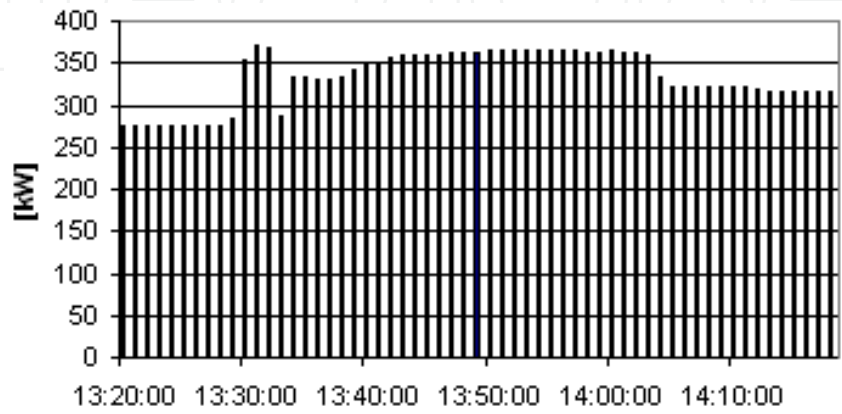


Fig. 27. Active power per phase 1 in the intermediate state (MV Line)

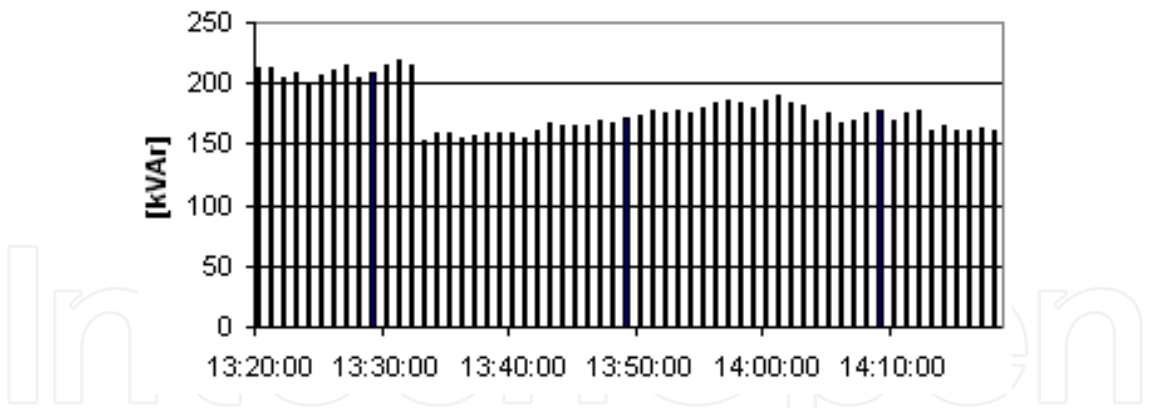


Fig. 28. Reactive power per phase 1 in the intermediate state (MV Line)

In the time period 13:20 - 13:35, the values of reactive power per phase 1 are almost equal to the values of active power. As a result, the power factor per phase 1 is very poor in the time period 13:20 - 13:35 (fig.26).

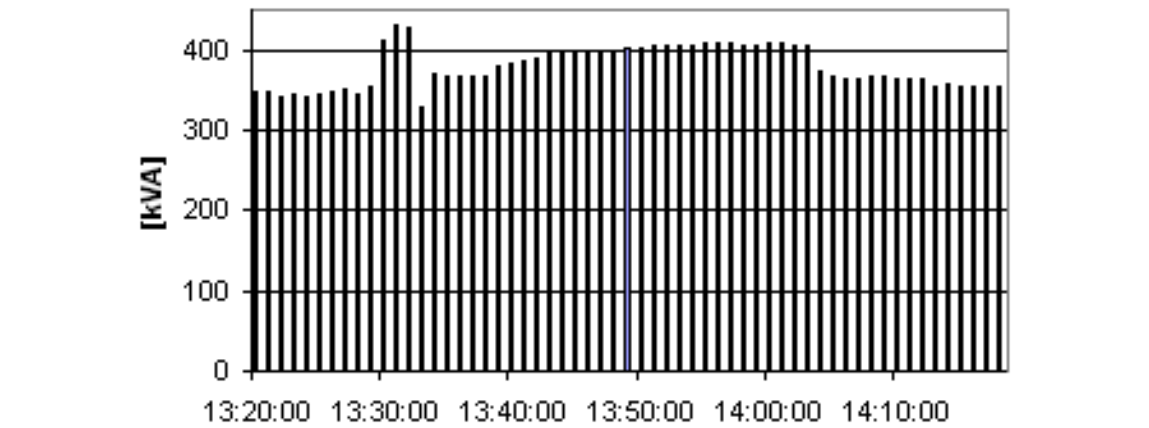


Fig. 29. Apparent power per phase 1 in the intermediate state (MV Line)

Fig.30-37 show the recorded parameters in the last stage of the heating. The furnace charge was totally melted in the recording period, 18:02-18:12.

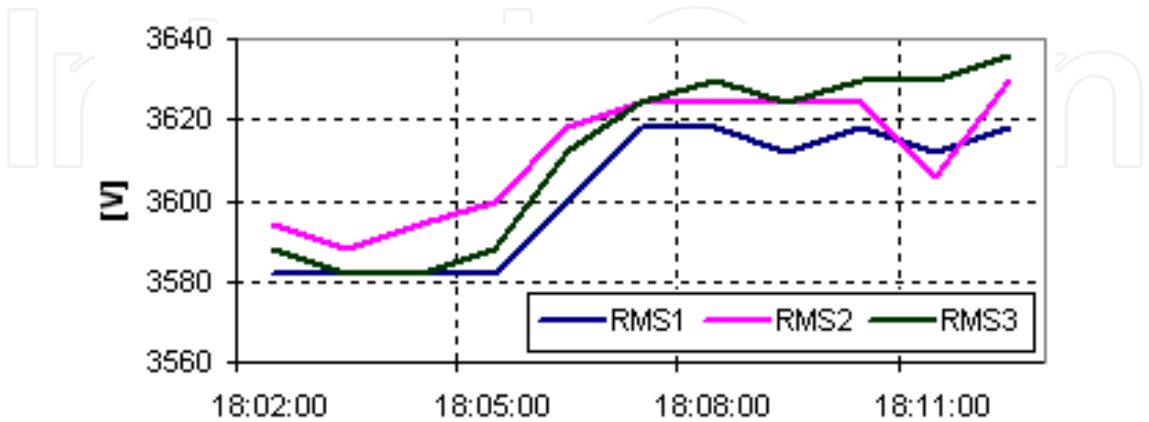


Fig. 30. RMS values of phase voltages in the last stage of the melting process (MV Line)

In the last stage of the melting process, THD of phase voltages are within compatibility limits, being smaller comparatively with the cold state or the intermediate state.

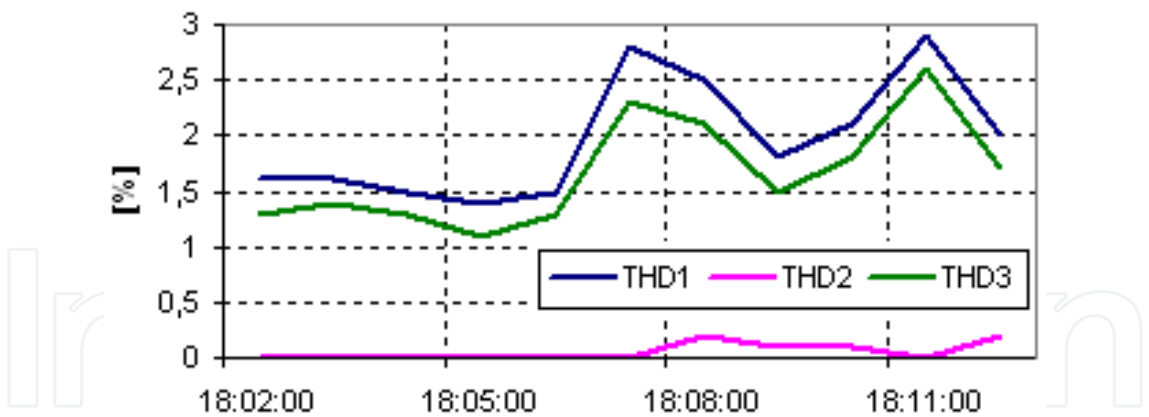


Fig. 31. THD of phase voltages in the last stage of the melting process (MV Line)

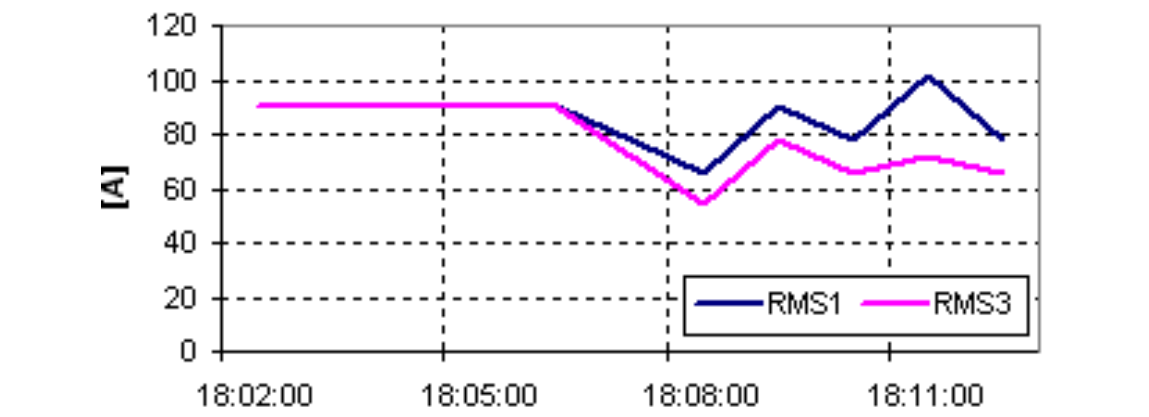


Fig. 32. RMS values of line currents in the last stage of the melting process (MV Line)

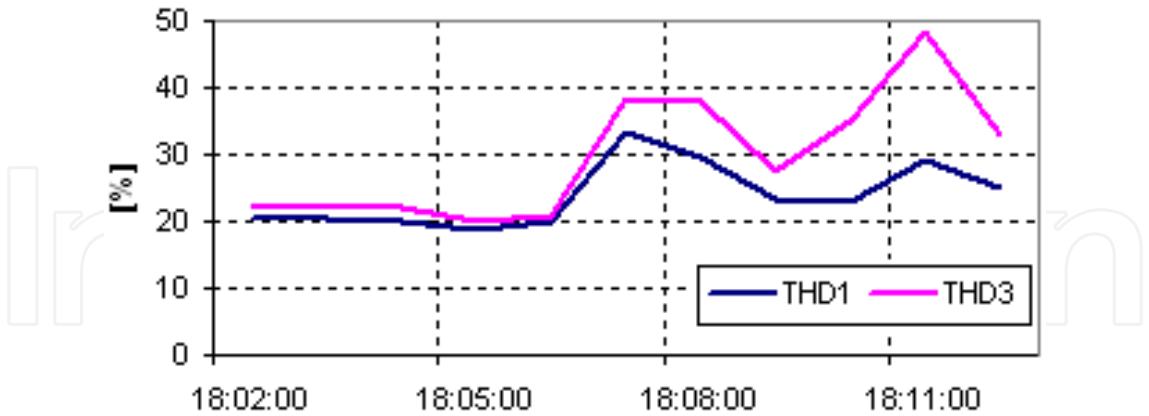


Fig. 33. THD of line currents in the last stage of the melting process (MV Line)

At the end of the melting process, the RMS values of line currents are much closer comparatively with cold state or intermediate state. THD of line currents exceed the compatibility limits, being of 20%...50% during this recording period. The difference between the power factor and the displacement factor is small in the last stage of the melting process (fig.34). This indicates a decrease of harmonic disturbances and reactive power consumption (fig.36), comparatively with the cold state or the intermediate state.

In the time period 18:07 - 18:12, the values of reactive power per phase 1 increase; consequently, the power factor and the displacement factor per phase 1 decrease. Recorded values of active power per phase 1 are close to the apparent power values.

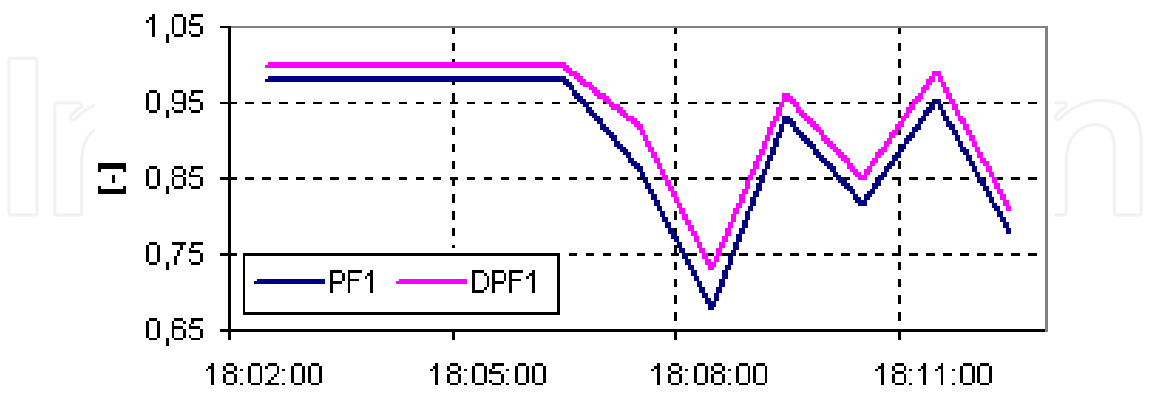


Fig. 34. DPF and PF per phase 1 in the last stage of the melting process (MV Line)

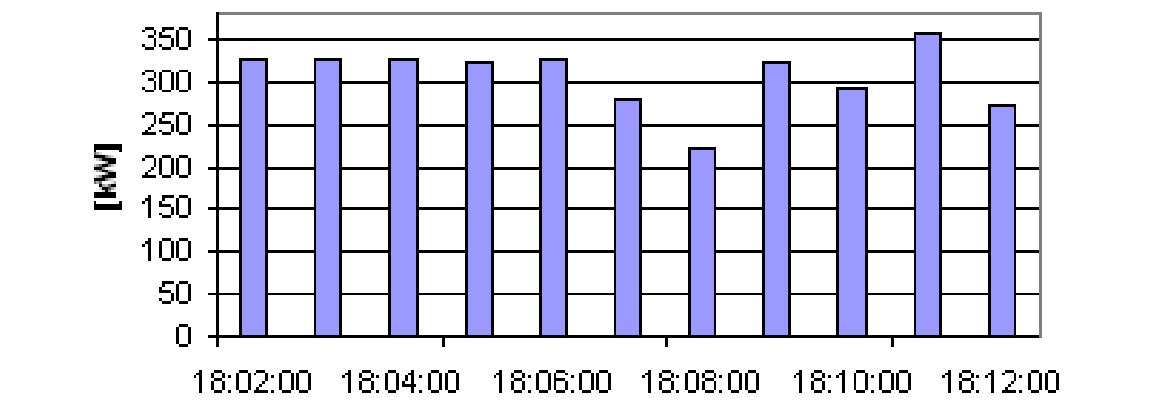


Fig. 35. Active power per phase 1 in the last stage of the melting process (MV Line)

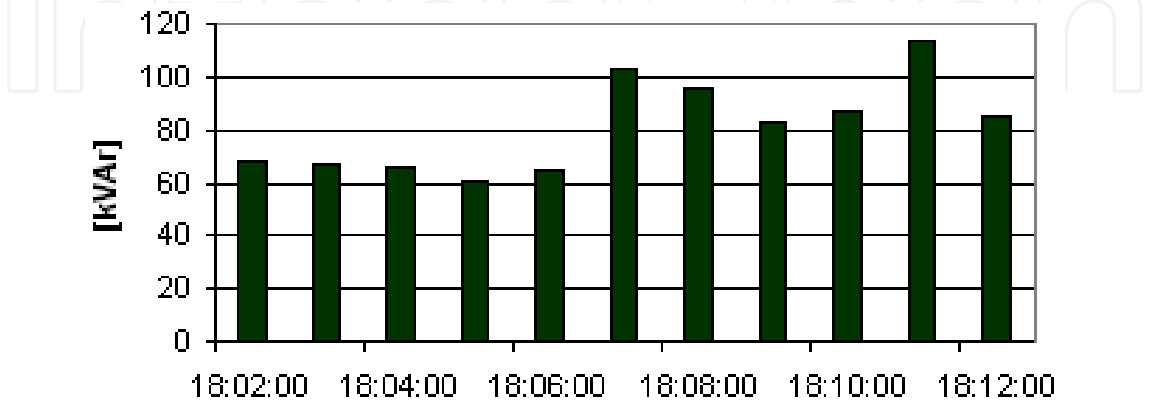


Fig. 36. Reactive power per phase 1 in the last stage of the melting process (MV Line)

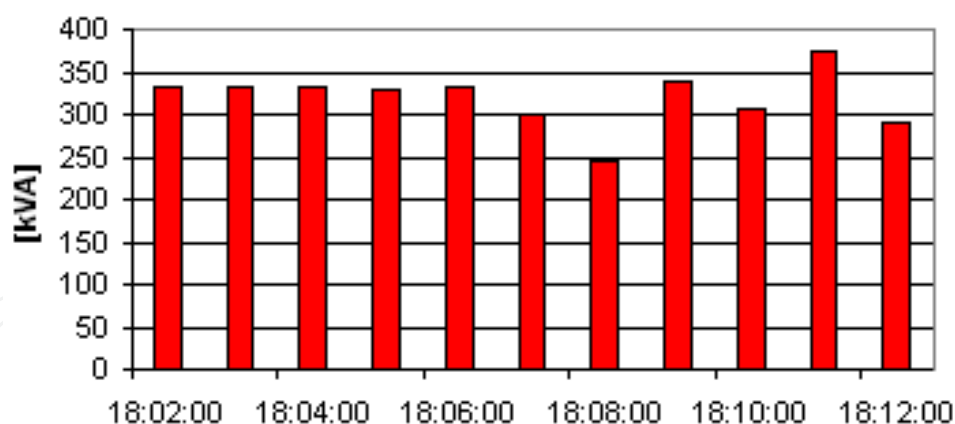


Fig. 37. Apparent power per phase 1 in the last stage of the melting process (MV Line)

6. Conclusion

The measurements results show that the operation of the analyzed furnace determines interharmonics and harmonics in the phase voltages and harmonics in the currents absorbed from the network.

THD of phase voltages are within compatibility limits, but voltage interharmonics exceed the compatibility limits in all the analyzed situations.

THD of line currents exceed the compatibility limits in all the heating stages. Because I_{THD} exceed 30%, which indicates a significant harmonic distortion, the probable malfunction of system components would be very high.

THD of line currents are bigger in intermediate state comparatively with the cold state, or comparatively with the end of melting. This situation can be explained by the complex and strongly coupled phenomena (eddy currents, heat transfer, phase transitions) that occur in the intermediate state.

Harmonics can be generated by the interaction of magnetic field (caused by the inductor) and the circulating currents in the furnace charge.

Because the furnace transformer is in Δ/Y connection, the levels of the triple-N harmonics currents are much smaller on MV Line versus LV Line. These harmonics circulate in the winding of transformer and do not propagate onto the MV network.

On MV Line, 5th and 25th harmonics currents exceed the compatibility limits. The levels of these harmonics are higher on MV Line versus LV Line. Also, THD of line currents and THD of phase voltages are higher on MV Line versus LV Line, in all the analyzed situations. The harmonic components cause increased eddy current losses in furnace transformer, because the losses are proportional to the square of the frequency. These losses can lead to early failure due to overheating and hot spots in the winding.

Shorter transformer lifetime can be very expensive. Equipment such as transformers is usually expected to last for 30 or 40 years and having to replace it in 7 to 10 years can have serious financial consequences.

To reduce the heating effects of harmonic currents created by the operation of analyzed furnace it must replaced the furnace transformer by a transformer with K-factor of an equal or higher value than 4.

Peak factors of line currents are high during the heating stages, and characterizes high transient overcurrents which, when detected by protection devices, can cause nuisance tripping.

The capacitors for power factor correction and the ones from Steinmetz circuit amplify in fact the harmonic problems.

PF is less than unity in all the analyzed situations. But, Steinmetz circuit is efficient only for unity PF, under sinusoidal conditions.

Under nonsinusoidal conditions, any attempt to achieve unity PF does not result in harmonic-free current. Similarly, compensation for current harmonics does not yield unity PF.

For optimizing the operation of analyzed induction furnace, it's imposing the simultaneous adoption of three technical measures: harmonics filtering, reactive power compensation and load balancing. That is the reason to introduce harmonic filters in the primary of furnace transformer to solve the power interface problems. In order to eliminate the unbalance, it is necessary to add another load balancing system in the connection point of the furnace to the power supply network.

7. References

- Arrillaga, J., Watson, N. R., & Chen, S. (2000). *Power System Quality Assessment*, John Wiley and Sons, ISBN 978-0-471-98865-6, New York.
- Ching-Tzong Su, Chen-Yi Lin, & Ji-Jen Wong (2008). Optimal Size and Location of Capacitors Placed on a Distribution System. *WSEAS Transactions on Power Systems*, Vol. 3, Issue 4, (april 2008), pp. 247-256, ISSN 1790-5060.
- George, S., & Agarwal, V. (2008). Optimum Control of Selective and Total Harmonic Distortion in Current and Voltage Under Nonsinusoidal Conditions, *IEEE Transactions on Power Delivery*, Vol.23, Issue 2, (april 2008), pp. 937-944, ISSN 0885-8977.
- De la Rosa, F. C. (2006). *Harmonics and Power Systems*, CRC Press, Taylor&Francis Group, ISBN 0-8493-30-16-5, New York.
- Iagăr, A., Popa, G. N., & Sora I. (2009). Analysis of Electromagnetic Pollution Produced by Line Frequency Coreless Induction Furnaces, *WSEAS TRANSACTIONS on SYSTEMS*, Vol. 8, Issue 1, (january 2009), pp. 1-11, ISSN 1109-2777.
- Lattarulo, F. (Ed(s).). (2007). *Electromagnetic Compatibility in Power System*, Elsevier Science&Technology Books, ISBN 978-0-08-045261-6.
- Muzi, F. (2008). Real-time Voltage Control to Improve Automation and Quality in Power Distribution, *WSEAS Transactions on Circuit and Systems*, Vol. 7, Issue 4, (april 2008), pp. 173-183, ISSN 1109-2734.
- Nuns, J., Foch, H., Metz, M. & Yang, X. (1993). Radiated and Conducted Interferences in Induction Heating Equipment: Characteristics and Remedies, *Proceedings of Fifth European Conference on Power Electronics and Applications*, Brighton, UK., Vol. 7, pp. 194-199, september 1993.
- Panoiu, M., Panoiu, C., Osaci, M. & Muscalagiu, I. (2008). Simulation Result about Harmonics Filtering Using Measurement of Some Electrical Items in Electrical Installation on UHP EAF, *WSEAS Transactions on Circuit and Systems*, Vol. 7, Issue 1, (january 2008), pp. 22-31, ISSN 1109-2734.
- Rudnev, V., Loveless, D., Cook, R., & Black, M. (2002). *Handbook of Induction Heating*, CRC Press, Taylor&Francis Group, ISBN 0824708482, New York.
- Sekara, T. B., Mikulovic, J.C., & Djuriscic, Z.R. (2008). Optimal Reactive Compensators in Power Systems Under Asymmetrical and Nonsinusoidal Conditions, *IEEE*

Transactions on Power Delivery, Vol. 23, Issue 2, (april 2008), pp. 974-984, ISSN 0885-8977.

CA8334, Three Phase Power Quality Analyser, technical handbook, Chauvin Arnoux, France, 2007.

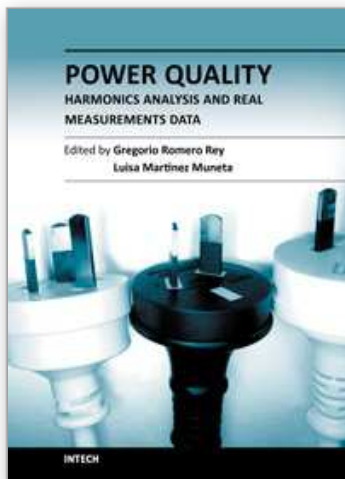
IEC 61000-3-4, EMC, Part 3-4: Limits – Limitation of Emission of Harmonic Currents in Low-Voltage Power Supply Systems for Equipment with Rated Current Greater than 16A, 1998.

IEC/TR 61000-3-6, EMC, Part 3-6: Limits – Assessment of Harmonic Emission Limits for the Connection of Distorting Installations to MV, HV and EHV Power Systems (revision), 2005.

Power Quality for Induction Melting in Metal Production, TechCommentary Electric Power Research Institute (EPRI), U.S.A., 1999, available at:

http://www.energy.ca.gov/process/pubs/pq_inductn_melting_tc114625.pdf

IntechOpen



Power Quality Harmonics Analysis and Real Measurements Data

Edited by Prof. Gregorio Romero

ISBN 978-953-307-335-4

Hard cover, 278 pages

Publisher InTech

Published online 23, November, 2011

Published in print edition November, 2011

Nowadays, the increasing use of power electronics equipment origins important distortions. The perfect AC power systems are a pure sinusoidal wave, both voltage and current, but the ever-increasing existence of non-linear loads modify the characteristics of voltage and current from the ideal sinusoidal wave. This deviation from the ideal wave is reflected by the harmonics and, although its effects vary depending on the type of load, it affects the efficiency of an electrical system and can cause considerable damage to the systems and infrastructures. Ensuring optimal power quality after a good design and devices means productivity, efficiency, competitiveness and profitability. Nevertheless, nobody can assure the optimal power quality when there is a good design if the correct testing and working process from the obtained data is not properly assured at every instant; this entails processing the real data correctly. In this book the reader will be introduced to the harmonics analysis from the real measurement data and to the study of different industrial environments and electronic devices.

How to reference

In order to correctly reference this scholarly work, feel free to copy and paste the following:

Angela Iagăr (2011). Power Quality Problems Generated by Line Frequency Coreless Induction Furnaces, Power Quality Harmonics Analysis and Real Measurements Data, Prof. Gregorio Romero (Ed.), ISBN: 978-953-307-335-4, InTech, Available from: <http://www.intechopen.com/books/power-quality-harmonics-analysis-and-real-measurements-data/power-quality-problems-generated-by-line-frequency-coreless-induction-furnaces>

INTECH
open science | open minds

InTech Europe

University Campus STeP Ri
Slavka Krautzeka 83/A
51000 Rijeka, Croatia
Phone: +385 (51) 770 447
Fax: +385 (51) 686 166
www.intechopen.com

InTech China

Unit 405, Office Block, Hotel Equatorial Shanghai
No.65, Yan An Road (West), Shanghai, 200040, China
中国上海市延安西路65号上海国际贵都大饭店办公楼405单元
Phone: +86-21-62489820
Fax: +86-21-62489821

© 2011 The Author(s). Licensee IntechOpen. This is an open access article distributed under the terms of the [Creative Commons Attribution 3.0 License](https://creativecommons.org/licenses/by/3.0/), which permits unrestricted use, distribution, and reproduction in any medium, provided the original work is properly cited.

IntechOpen

IntechOpen